

# Theoretical Investigation of the Charge Injection Effects on the Electronic Properties of Substituted Oligodiacetylenes

Massimo Ottonelli,\* Gianfranco Musso, Davide Comoretto, and Giovanna Dellepiane

INFM-INSTM-Università di Genova, Dipartimento di Chimica e Chimica Industriale,  
Via Dodecaneso 31, I-16146 Genova, Italy

Received: April 6, 2004; In Final Form: June 3, 2004

We discuss the charge-induced modifications in the ground state geometry and in the electronic properties of two types of fully carbazolyl-substituted oligodiacetylenes, named  $CBD_n$  and  $CHD_n$  respectively, which are taken as models of the corresponding polymers. Quantum chemical calculations have been performed on the isolated oligomers carrying substituents, either directly linked to the backbone ( $CBD_n$ ) or connected to it through a methylene spacer ( $CHD_n$ ). The collective electronic oscillator (CEO) approach is used to compute the excitations in terms of the one-electron transition density matrixes (CEO-modes). The simulated photoinduced absorption spectra which are obtained show interesting features, and the allowed low-energy transitions compare favorably with experimental results where available. Two-dimensional plots in real space of the CEO-modes allow us to analyze the physical nature of the excitons in terms of the photoinduced electron/hole pairs motion. For charged oligomers, two different types of electronic interactions between the  $\pi$  systems of the backbone and of the substituents are seen to occur in the two types of oligomers. Even in the presence of a methylene spacer, a charge flow is unexpectedly observed from the backbone toward the carbazolyl substituents, and a manifold of allowed low-energy excitations rises. In this way, the experimental peaks in the photoinduced absorption spectra of polyDCHD (the polymer corresponding to  $CHD_n$ ) find a new explanation, which is different from (and more convincing than) that previously given by us on the basis of results obtained on unsubstituted oligomers.

## 1. Introduction

Organic conjugated materials have achieved increasing importance in the development of new devices for a wide variety of technological applications,<sup>1</sup> e.g., organic light emitting diodes (LED's),<sup>2,3</sup> light emitting electrochemical cells and solar cells,<sup>4</sup> photodiodes,<sup>5</sup> or field effect transistors (FET).<sup>6</sup> The photo- and physicochemical properties of these materials, whose knowledge is fundamental for the development of devices, are very complex due to the many types of processes involved. For example, photoexcitation could occur through different types of channels involving, e.g., singlet or triplet excitons or charge-separation states, and on the other hand charge transport and recombination processes are strictly correlated to the stability of the charge-induced geometry relaxation. Knowledge of these processes is important for understanding the mobility of the charge induced defects and their recombination in real devices such as LEDs<sup>7</sup> or (as recently demonstrated) electrochemical actuators.<sup>8</sup>

This complexity forms an interesting subject for theoretical investigation trying to understand the relationships between the molecular geometry and the electronic properties, to help in developing new conjugated materials showing improved technological properties. For these reasons, a wide number of theoretical and experimental studies has been dedicated to this matter. Due, however, to the large computational size of the systems involved, most theoretical work is focused on unsubstituted oligomers or polymers. This implies neglecting the possible interactions between the  $\pi$  system of the backbone and the substituents, either because they are implicitly assumed to be small or because the lower excitations of the substituted

systems are believed to essentially belong to the  $\pi$  system of the backbone. On the other hand, experiments are frequently carried out on substituted systems, which can render the comparison with the theoretical results often questionable.

What we want to do here is to contribute to throw light on these problems, taking advantage of the opportunities given by a recent theoretical approach, the CEO method,<sup>9,10</sup> to study the electronic properties of fairly large substituted systems in a way which explicitly takes into account the possible interactions between the conjugated backbone and the substituents. We consider doubly positive photoexcitons induced by charge injection on oligomers of a particular class of polydiacetylenes that are interesting materials for their large off-resonance optical nonlinearities and as models of rodlike systems.<sup>11,12</sup> The general formula of the carbazolyl-substituted oligodiacetylenes studied is given in Figure 1. When the chromophore groups are directly linked to the backbone, we have the  $n$ -oligomer of the 1,4-bis-(N-carbazolyl)-1,3-butadiyne (named  $CBD_n$ ), whereas when a methylene spacer is present, we have the  $n$ -oligomer of the 1,6-bis-(N-carbazolyl)-2,4-hexadiyne (named  $CHD_n$ ). Polycarbazolyl-diacetylenes of these and other types have been long characterized and studied in our laboratory.<sup>13</sup> In the following,  $n$  takes the values 2, 4, and 6.

## 2. Theory and Computational Details

The electronic excitations have been computed using the collective electronic oscillator (CEO) method on the basis of the AM1<sup>14</sup> optimized ground-state geometries obtained using the MOPAC<sup>15</sup> code. The AM1 Hamiltonian is known to be well suited to reproduce with good accuracy the ground-state geometries of large-sized organic systems.<sup>16</sup>

\* To whom correspondence should be addressed. Tel: +39-010-353-8703. Fax: +39-010-353-6199. E-mail: massimo@chimica.unige.it.

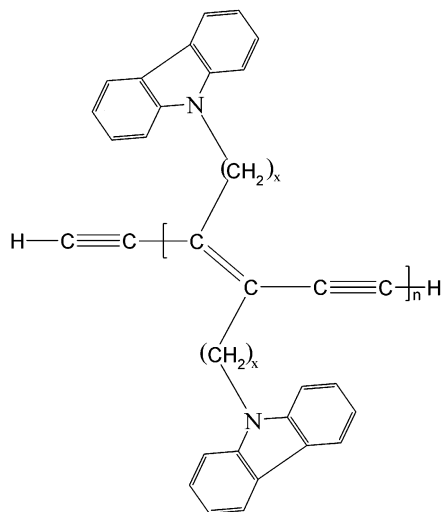


**Figure 1.** Molecular structure of the  $\text{CBD}_n$  ( $x = 0$ ) and  $\text{CHD}_n$  ( $x = 1$ ) oligomers.

The CEO technique<sup>17</sup> was developed in the time-dependent Hartree–Fock (TDHF) framework, in which it is assumed that the many-electron wavefunction  $\Psi(t)$ , describing the molecular system when perturbed by an external time-dependent field, is represented at all times by a single Slater determinant. In this approach, however, one does not directly seek the excited electronic wavefunctions but only the one-electron transition density matrixes,<sup>17,18</sup> which are named the electronic modes  $\xi_a$  (to which correspond the excitation energies  $\Omega_a$ ). This choice allows us to sensibly increase the dimension of the basis set that can be used in the calculations and, consequently, the size of the chemical system which can be studied. Knowledge of the ordered pairs  $(\Omega_a, \xi_a)$  is all we need for the evaluation of the linear optical response through the calculation of the dynamic polarizability  $\alpha(\omega)$ <sup>17,18</sup>

$$\alpha(\omega) = \sum_a \alpha_a(\omega) = \frac{2}{3} \sum_a \frac{\Omega_a \text{Tr}(\bar{\mu} \xi_a)^* \text{Tr}(\bar{\mu} \xi_a)}{\Omega_a^2 - (\omega + i\Gamma_a)^2} \quad (2.1)$$

where  $\Gamma_a$  is the dephasing rate for the excited state  $a$ .

The optimized ground state geometries of the neutral and doubly positively charged oligomers, obtained using the MO-PAC code without any symmetry constraint, are used as an input for the CEO code developed by the Mukamel's group,<sup>19</sup> where the CEO procedure is implemented on the basis of a semiempirical INDO/S Hamiltonian.<sup>20</sup> [At present we consider only doubly charged systems because we are using a restricted Hartree–Fock procedure.] The original parameters of the INDO Hamiltonian<sup>21</sup> were reoptimized by the Zerner's group in order to reproduce the electronic spectra of organic molecules.<sup>22</sup> In eq 2.1, the number of modes considered has been 60 for the neutral and 80 for the charged oligomers and the corresponding oscillator strengths have been also computed according to the expression  $f_a = (2/3)\Omega_a \text{Tr}(\bar{\mu} \xi_a)^* \text{Tr}(\bar{\mu} \xi_a)$ . The optical spectrum  $\mathcal{J}(\omega)$  has been obtained through the expression

$$\mathcal{J}(\omega) \propto \sum_a \text{Im}[\alpha_a(\omega)] \quad (2.2)$$

where a common value of 0.03 eV is assumed for all the dephasing rate coefficients ( $\Gamma_a$ ).

The plots of the calculated one-electron transition density matrixes  $\xi_a$  contracted over the atoms, that is, in the real space, give a representation of the electron–hole pairs motions induced

by the photon absorption during the excitation process. This allows us to correlate the electron density variations with the optical and topological properties of the molecular systems studied and can give information on the molecular design of new structures. In the two-dimensional plots, where the  $x$  ( $y$ ) axis represents electrons (holes) on an atom, diagonal elements  $(\xi_a)_{rr}$  are related to the net photoinduced charge on the  $r$ th atom, while the off-diagonal element  $(\xi_a)_{rs}$  represents the probability of finding an electron and a hole on the  $r$ th and  $s$ th atom, respectively. So the difference between the values of two symmetrical off-diagonal elements gives information about the probability and the direction of charge transfer between the  $r$ th and  $s$ th atom.

### 3 Results and Discussion

**3.1. Geometries and Charge Distributions.** The AM1 bond lengths, computed without forcing any symmetry constraint, for the neutral and charged oligomers are shown in Tables 1 and 2 for the backbone and carbazoyl moieties, respectively. The reported carbazoyl bond lengths are mean values over  $n$  and over all the substituents belonging to a given oligomer, the overall standard deviation being less than  $\pm 0.001$  Å.

In the neutral case, only the backbone bond lengths for the largest oligomers considered ( $n = 6$ ) are reported, because no particular variations occur with increasing  $n$ . In  $\text{CHD}_6$ , the triple bonds are longer than in  $\text{CBD}_6$ , whereas the opposite occurs for double and single bonds. From Table 2, it is seen that in the two types of neutral oligomers the geometries of the carbazoyl moieties are very close to each other, with the only exception of the bonds springing from the N atoms. Of these, the bonds directly involved in the carbazoyl  $\pi$  system (labeled h in the Table) are longer in  $\text{CBD}_6$  (by 0.014 Å), and the reverse is true (by  $-0.015$  Å) for the bond, labeled i, connecting the substituent to the backbone. With the AM1 bond lengths for isolated  $\text{C}\equiv\text{C}$ ,  $\text{C}=\text{C}$ , and  $\text{C}-\text{C}$  being 1.195, 1.339, and 1.536 Å, respectively, the results in Table 1 indicate that for  $\text{CBD}_n$  two somewhat concurrent conjugation pathways are effective. The first one runs over the whole  $\pi$  system of the backbone, whereas the second includes two neighbor carbazoyl moieties connected by a backbone double bond. For  $\text{CHD}_n$ , a comparison with the bond lengths of the unsubstituted oligomer<sup>23</sup> (1.202 Å for  $\text{C}\equiv\text{C}$ , 1.350 Å for  $\text{C}=\text{C}$  and 1.402 Å for  $\text{C}-\text{C}$ ) shows that the presence of the spacer almost prevents any *direct* interaction between the two moieties. The computed values compare favorably (especially for  $\text{CHD}_n$ ) with the experimental backbone structure of a similarly substituted polydiacetylene<sup>24</sup> (1.21, 1.36, and 1.41 Å for the triple, double, and single CC bonds, respectively). Finally a last point deserves mention. Although not reported in the table, strong variations ( $50^\circ$ – $75^\circ$ ) are obtained for the backbone dihedral angles with respect to the ideal values ( $180^\circ$ ) valid for the unsubstituted oligomer  $\text{C}_{2h}$  structure, due to the presence of the carbazoyl moieties. The largest deviations are found for  $\text{CBD}_n$  and in general near the chain ends. Increasing the oligomer size seems to slightly reduce these variations, an effect that can be expected to continue for larger oligomers ( $n \gg 6$ ) due to the backbone conjugation. In this respect, it is important to stress that, despite the nonplanar backbone structure, in both  $\text{CBD}_n$  and  $\text{CHD}_n$  the presence in the triple bonds of *two orthogonal*  $\pi$  bonds allows a considerable extent of conjugation with the  $\pi$  electrons of the neighbor double bonds.

For doubly charged oligomers, the bond length differences are enhanced, and a number of somewhat unexpected features emerge. First, for  $\text{CHD}_n$ , the backbone bond lengths are



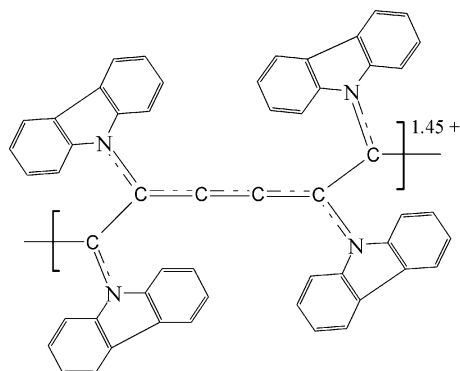


**Figure 2.** Schematic picture of the local charged induced structure in  $\text{CBD}_n$  oligomers.

**TABLE 3: Charge Excess Distribution (%) in  $\text{CBD}_n$  and  $\text{CHD}_n$  Doubly Charged Oligomers**

$n$	$\text{CBD}_n$			$\text{CHD}_n$		
	2	4	6	2	4	6
backbone	23.35	25.28	17.17	6.90	5.60	5.05
carbazole moieties (total)	76.65	74.72	82.83	93.10	94.40	94.95
I <sup>a</sup>	29.65	5.92	1.16	23.87	17.50	12.25
II	9.15	2.00	0.50	23.47	11.70	16.89
III	8.50	21.80	1.55	23.82	12.28	1.05
IV	29.35	4.50	1.96	21.94	8.30	0.10
V		7.90	6.25		4.70	3.20
VI		23.10	1.84		6.80	12.45
VII		2.35	23.00		14.85	1.85
VIII		7.15	7.64		18.30	11.38
IX			6.07			13.09
X			26.15			2.30
XI			2.28			14.45
XII			4.43			5.95

<sup>a</sup> For the numbering of carbazolyl units in the oligomers, see Figure 3.

In Table 3, the distribution of the excess charge among the backbone and the carbazolyl groups is displayed (see Figure 3 for the substituents numbering). For  $\text{CHD}_n$ , a very small fraction ( $\leq 7\%$ ) of the excess charge is located on the backbone (a result which is confirmed by an ab initio RHF/6-31G optimization on  $\text{CHD}_2$ ), and the rest is spread over all carbazolyl units, which explains the small geometry relaxations found in this type of

oligomer. For  $\text{CBD}_n$  too, the fraction of charge on the backbone turns out to be small ( $\leq 25\%$ ), and in both cases it basically decreases with increasing oligomer size. The relative positions of the INDO energies of the HOMOs of carbazole ( $-7.70$  eV) and of the unsubstituted  $n = 6$  oligomer ( $-6.88$  eV) would suggest that it should be easier to extract an electron from the backbone. If, however, the calculations of the HOMO energies are performed at the actual geometries of the moieties in neutral  $\text{CBD}_6$  ( $\text{CHD}_6$ ), the results are  $-7.62$  ( $-7.62$ ) eV for carbazole and  $-8.73$  ( $-8.27$ ) eV for the backbones, due to the distortions mainly in the backbone dihedral angles caused by the carbazolyl interactions. The delocalization of an appreciable fraction of the excess charge on the backbone in  $\text{CBD}_n$  is only made possible by the already referred to conjugation effects involving the lone pairs of the N atoms. An analysis of the distribution of the excess charge among the carbazolyl groups shows that for  $\text{CBD}_n$  the majority of the charge is concentrated on the units belonging to the bipolaronic structure located toward one end of the chain, whereas for  $\text{CHD}_n$ , it is essentially equally distributed over the units at the chain ends. The latter results are consistent with those previously obtained by us<sup>25</sup> and by other authors<sup>26</sup> on unsubstituted oligodiacylenes and oligophenylenes, respectively. It seems likely that in truly one-dimensional cases the bipolaron splits into two singlet polarons<sup>27</sup> only for extended  $\pi$  systems, whereas in the presence of carbazolyl substituents, the injected charge spreads over the latter moieties already for short oligomers. Otherwise, for  $\text{CBD}_n$ , which can be seen as a two-dimensional conjugated  $\pi$  system, the transverse conjugation stabilizes the bipolaron structure.

Finally in Figure 4, we report, as an example, a picture of the optimized structures for the neutral and doubly charged  $\text{CBD}_6$  and  $\text{CHD}_6$  oligomers. It seems likely that for charged  $\text{CBD}_6$  the location of the charge-induced defect and its morphology remind the structure of cis 2-butene, and that for both oligomers the carbazolyl moieties assume a helical arrangement.

**3.2. Excited States and Absorption Spectra.** The theoretical absorption spectra, calculated as specified in section 2, are shown in Figure 5 for neutral oligomers, as well as in Figure 7 for the doubly charged ones. We remind that we are using a kind of restricted Hartree–Fock procedure, and consequently, only singlet excitations are obtained. Moreover, with the number

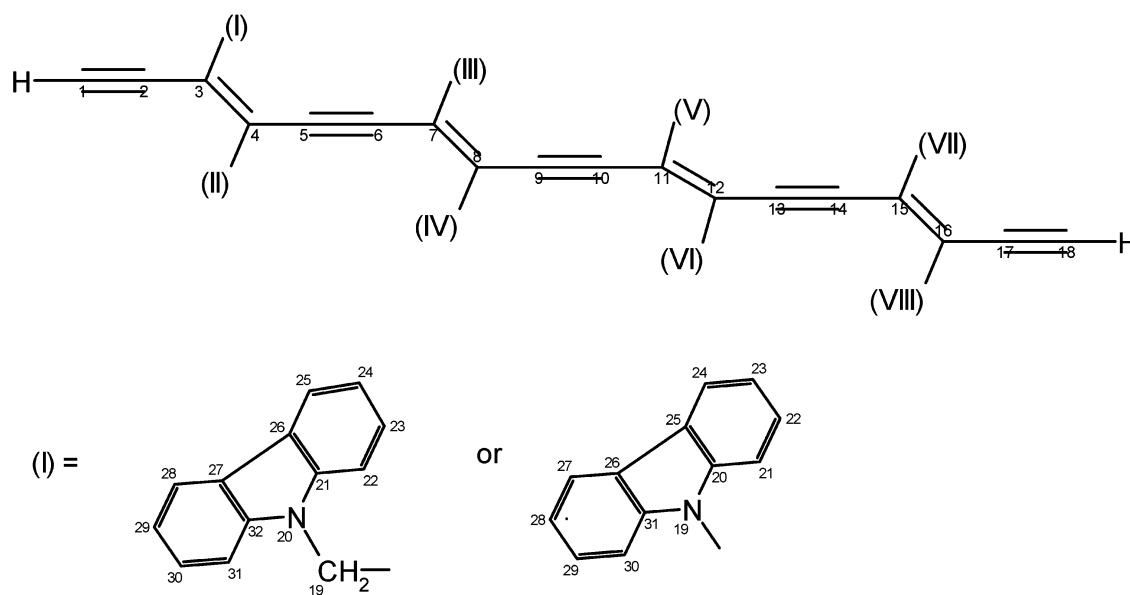


**Figure 3.** Atom numbering in the backbone and in the carbazolyl units in  $\text{CHD}_4$  and  $\text{CBD}_4$  oligomers.



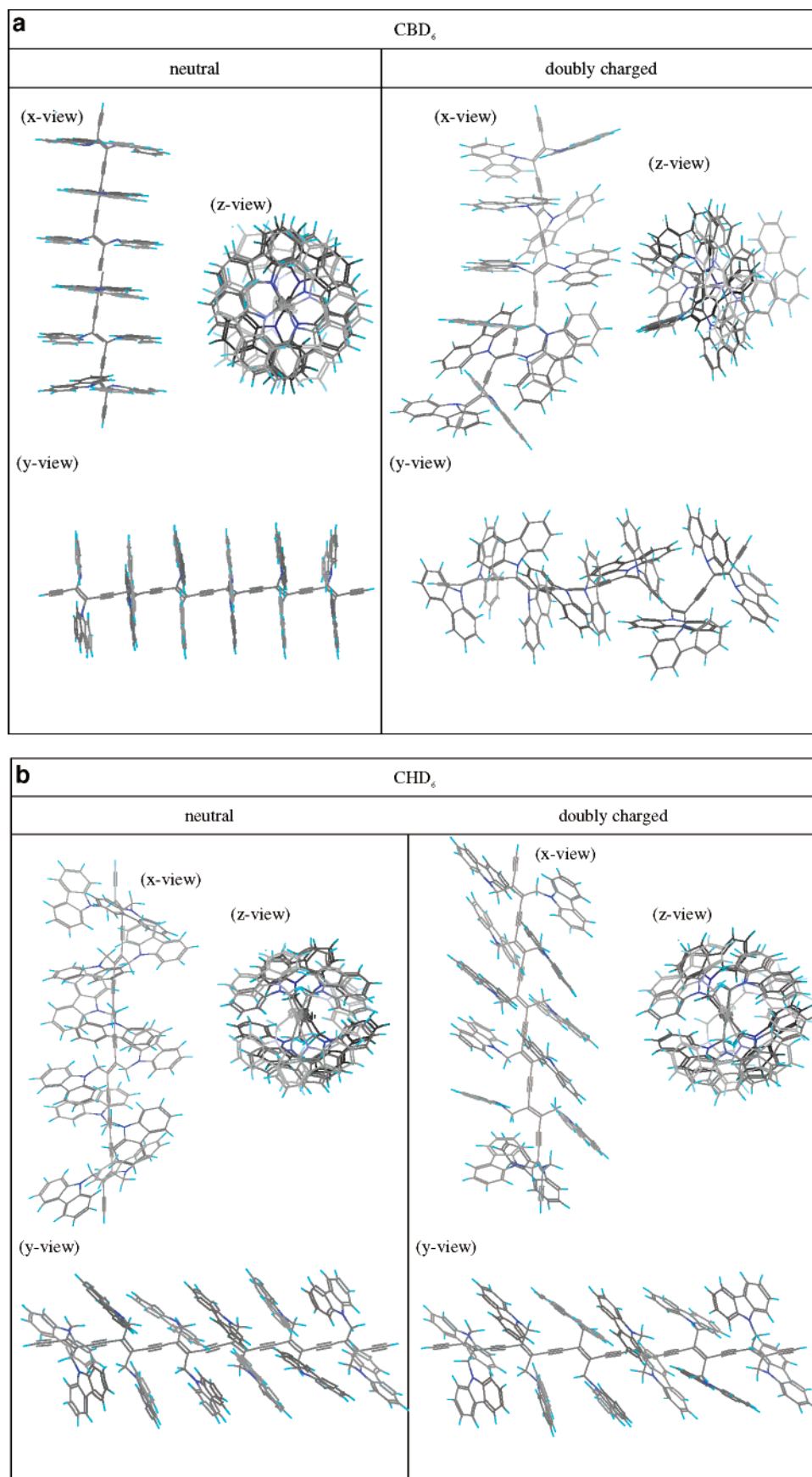


**Figure 4.** (a) AM1 ground-state optimized geometries for the  $\text{CBD}_6$  (a) and  $\text{CHD}_6$  (b) oligomers. (b) AM1 ground-state optimized geometries for the  $\text{CBD}_6$  (a) and  $\text{CHD}_6$  (b) oligomers.

of CEO modes for each case being fixed in advance, the scanned energies window in the absorption spectra results to be reduced

as the oligomer size increases. As a consequence for the larger oligomers ( $n = 6$  for the neutral and  $n \geq 4$  for the charged

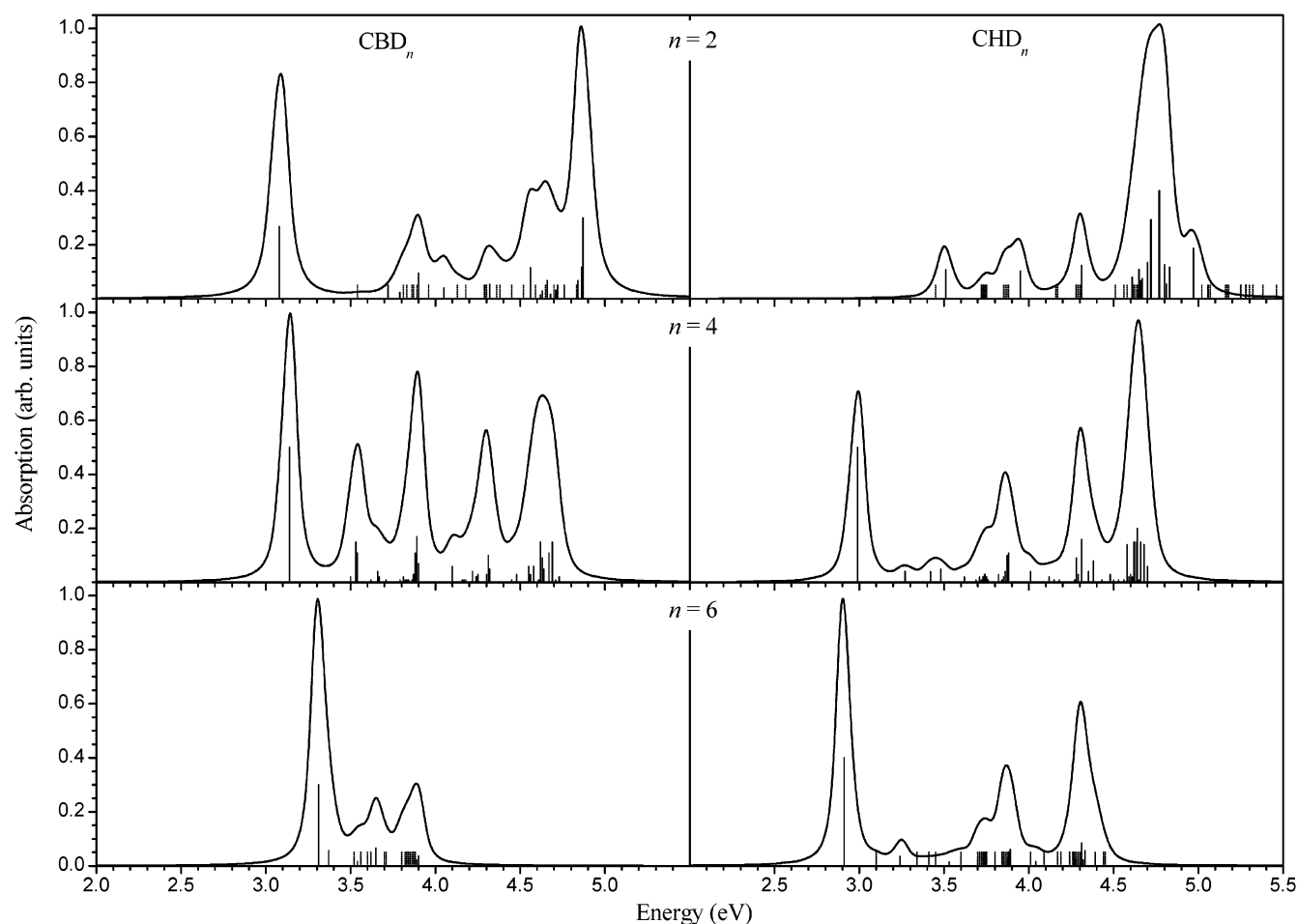


**Figure 5.** Computed absorption spectra for the neutral  $\text{CBD}_n$  and  $\text{CHD}_n$  oligomer. Proportional stick spectra are also reported, where solid (dotted) lines represent allowed (dark) transitions. Each spectrum is normalized to its highest peak.

ones), the higher excitations, which are mostly associated with the carbazolyl moiety, cannot be considered.

In Figure 5, the lowest allowed transition, which will be shown below to be correlated to a backbone excitation, is seen to follow an opposite behavior in the two types of oligomers. The transition blue-shifts with increasing oligomer size in  $\text{CBD}_n$  (3.08, 3.14, and 3.31 eV for  $n = 2, 4$ , and  $6$ , respectively) and red-shifts in  $\text{CHD}_n$  (3.51, 2.99, and 2.91 eV, respectively). Both series (with the exception of  $\text{CBD}_2$ ) are blue-shifted with respect to the corresponding unsubstituted oligomers, which give<sup>28</sup> 3.34, 2.84, and 2.65 eV. This behavior is correlated to the different conjugation lengths in the three types of oligomers. For the unsubstituted oligomer, the total trans geometry allows the most efficient and wide conjugations path,<sup>29</sup> whereas the presence of dihedral angles different from  $180^\circ$  in  $\text{CBD}_n$  and  $\text{CHD}_n$ , and the alternative conjugation pathway in  $\text{CBD}_n$ , reduce the conjugation length of the backbone, as underlined by the plots of the corresponding CEO modes in Figure 6. Only the backbone moieties are displayed in the plots, since for the above transitions small interactions with the carbazolyl substituents occur only in  $\text{CBD}_2$  (where their presence explains the lower excitation energy found with respect to the unsubstituted oligomer), whereas they are almost completely absent in the remaining cases. From Figure 6, it is seen that the conjugation length is drastically reduced in  $\text{CBD}_n$  with respect to  $\text{CHD}_n$  and to the unsubstituted oligomers<sup>23</sup> (not reported here), due to the fact that the largest deviations from the trans structure occur in  $\text{CBD}_n$ , as mentioned previously. Specifically, the conjugation length in  $\text{CBD}_n$  covers about two repeating units, nearly

independent of the oligomer size. Most important and despite the geometry distortion, in both systems, interaction between the  $\pi$  electrons of the double and triple bonds is seen to be still possible, due to the presence of two orthogonal  $\pi$  bonds in the latter. This interaction is apparent in the plot relative to  $\text{CBD}_6$  in the form of small off-diagonal elements in the region of the C atoms whose label is less than 18. A somewhat different situation, which resembles the unsubstituted case, is found in  $\text{CHD}_n$ , where the excitation involves the whole backbone, except perhaps the chain ends, and becomes more extended as  $n$  increases. In fact, it covers two, about three, and about four repeating units for the dimer, tetramer, and hexamer respectively, which accounts for the computed red-shift.

As a final detail in Figure 5, we finally note that for  $\text{CBD}_n$  new features appear in the region 3.5–4.0 eV with respect to the unsubstituted case, which are related to the interaction between the backbone and the carbazolyl moieties. On the contrary, for  $\text{CHD}_n$  to first order the computed spectra are the superposition of those of the unsubstituted oligomer and of carbazole, as shown in ref 29.

The calculated absorption spectra for the doubly charged case, which can be taken as a model for the photoinduced spectra, are shown in Figure 7 and allow for a few interesting remarks. For the unsubstituted doubly charged systems, the lowest transition energies were calculated at 2.76, 1.95, and 1.54 eV for  $n = 2, 4$ , and  $6$  respectively, and only for large  $n$  ( $\geq 12$ ), the two injected charges could evolve into an ensemble of two interacting polarons, which shows a very low excitation energy (for  $n = 15$ , 0.25 eV).<sup>28</sup> The corresponding values found for

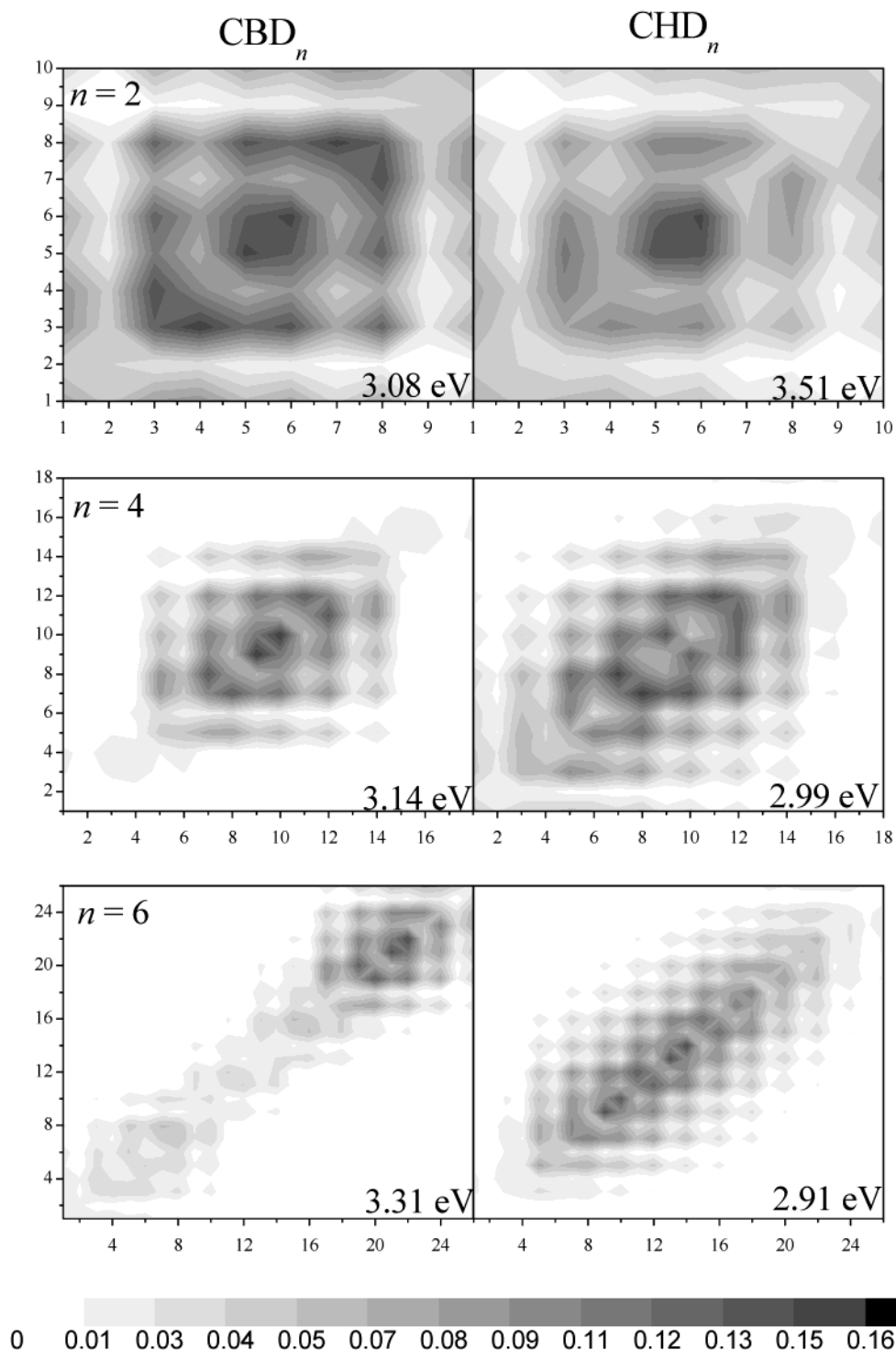


**Figure 6.** Partial contour plots (see text) of the CEO modes for the lowest optical transitions of the  $\text{CBD}_n$  and  $\text{CHD}_n$  neutral oligomers. Bottom: contour scale. The atom labeling is shown in Figure 3.

doubly charged  $\text{CBD}_n$  ( $\text{CHD}_n$ ) are 1.79 (0.34), 1.67 (0.68), and 0.63 (0.37) eV for  $n = 2, 4$ , and  $6$ , respectively. The latter transition energies are substantially red-shifted with respect to those of the unsubstituted molecule, and despite the short length of the present oligomers, they are comparable to the result for the large unsubstituted oligomer, especially in  $\text{CHD}_n$ .

For  $\text{CHD}_6$ , a peak at 2.3 eV is also present with an appreciable oscillator strength, a transition involving only the backbone which is correlated to the larger amount of trans structure in this oligomer.

Three points in the spectra of Figure 7 deserve a closer examination. First, the lowest excitation energy markedly

decreases with increasing  $n$  in  $\text{CBD}_n$ , and is almost constant for  $\text{CHD}_n$ . Second, for  $\text{CBD}_n$ , the lowest allowed excitation is set well apart from the higher transitions, whereas for  $\text{CHD}_n$ , a rather large manifold of allowed excitations close in energy is present, which makes the peaks more broadened. Third, the number of dark transitions results to be increased with respect to the neutral oligomers. To get insight on the above points, we report in Figure 8 the full plots of the CEO modes for the transitions referred to above. For  $\text{CBD}_n$ , the excitation is seen to be localized on the previously discussed butatrienic structure. We remind that such a structure, where an excess charge and a geometry relaxation are strictly connected, is usually called a

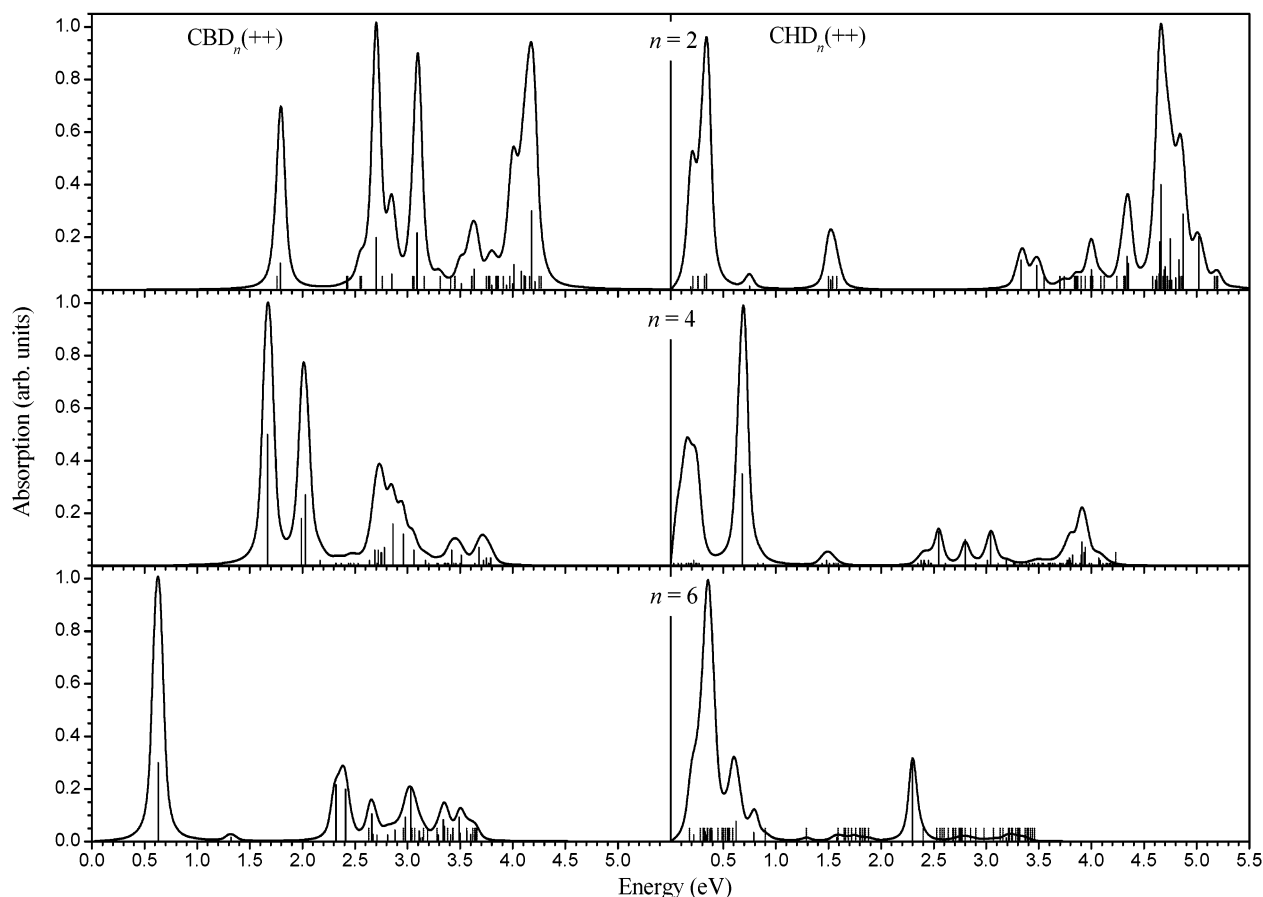


**Figure 7.** Computed absorption spectra for the doubly charged  $\text{CBD}_n$  and  $\text{CHD}_n$  oligomers. Proportional stick spectra are also reported, where solids (dotted) lines represent allowed (dark) transitions. Each spectrum is normalized to its highest peak.

bipolaron or a polaron according to its net global charge. Here interactions between the backbone and the carbazoyl units involved in this structure occur, as shown by the presence of off-diagonal terms in the plots. In the dimer, the excitation has a charge-transfer character (symmetrical off-diagonal elements have different weights), and electrons move from the backbone to the two carbazoyl units in positions II and III, which take part in the bipolaron (see Figure 3), whereas one of the less distorted carbazoyl moieties in position I is concerned with an opposite motion. Similar is the behavior of the tetramer, in which the carbazoyls involved in the bipolaron are in positions IV and V, but the amount of electron transfer toward the latter is somewhat larger, accounting for the slight red-shift of the transition with respect to the dimer. In the inset in the plot, the backbone is shown in detail, and the excitation is seen to be localized on the central section, that is, on the butatrienic structure, as was in the dimer, with small interactions with the remaining bonds. A different situation is found in  $\text{CBD}_6$ , where the excitation still includes a butatrienic structure but also extends over the rest of the backbone, and charge transfer occurs toward several carbazoyl moieties. These features give rise to the large red-shift in this oligomer. To be specific, for the two shorter oligomers, the excitation is dominated by the conjugation path involving one repeating unit and the two adjacent carbazoyls, whereas for the hexamer, such a moiety also interacts with the rest of the molecule, which resembles a neutral tetramer made more nearly planar. This picture clearly emerges from the inset in the plot and is in agreement with the geometry results of section 3.1, as well as with the discussion of the spectra of neutral  $\text{CBD}_n$ .

Contrary to what one could expect in view of the presence of the  $\text{CH}_2$  spacer, it is in the  $\text{CHD}_n$  series that the largest

redshifts with respect to the unsubstituted oligomers are predicted. The energy of the lowest excitation is seen to be practically independent of the oligomer size (the seeming deviation for  $\text{CHD}_4$  is due to the different nature of the transition chosen in this case,<sup>23</sup> see also below), the reason for this being that the excitation always involves the whole molecule. This behavior is apparent in the CEO plots and is the counterpart of what previously pointed out in the geometry section. In fact, contrary to  $\text{CBD}_n$ , for charged  $\text{CHD}_n$ , there is no bipolaronic structure, but the geometry relaxations are very limited as noted before, the largest effect being the decrease of the backbone dihedral angles toward planarity. In the dimer, the excitation does not carry an appreciable charge transfer character, and there is only a small probability of electron motion from the backbone to the carbazoyls. In the higher oligomers, however, interactions with several carbazoyl moieties occur, and in fact, already for  $\text{CHD}_4$  the backbone is completely involved (see inset) in interactions with carbazoyl units in positions IV to VIII. The charge-transfer character of the excitation is apparent, but in this case, *holes* are moving from the backbone to the substituents. The usual behavior is recovered, as could be expected, in the really lowest-energy transition of  $\text{CHD}_4$ ,<sup>29</sup> as well as in  $\text{CHD}_6$ , where electrons move toward the carbazoyls and in fact the transition energy decreases.

The above results suggest that the latter type of oligomers could be seen, to a first approximation (at least for the excitations below 1.0 eV), as distorted unsubstituted oligomers interacting with a neighborhood of partially charged carbazole molecules. We can recall at this point that the  $\text{CHD}_4$  results exhibit a great similarity<sup>29</sup> with the experimental data of the photoinduced absorption spectrum of the corresponding polymer, namely



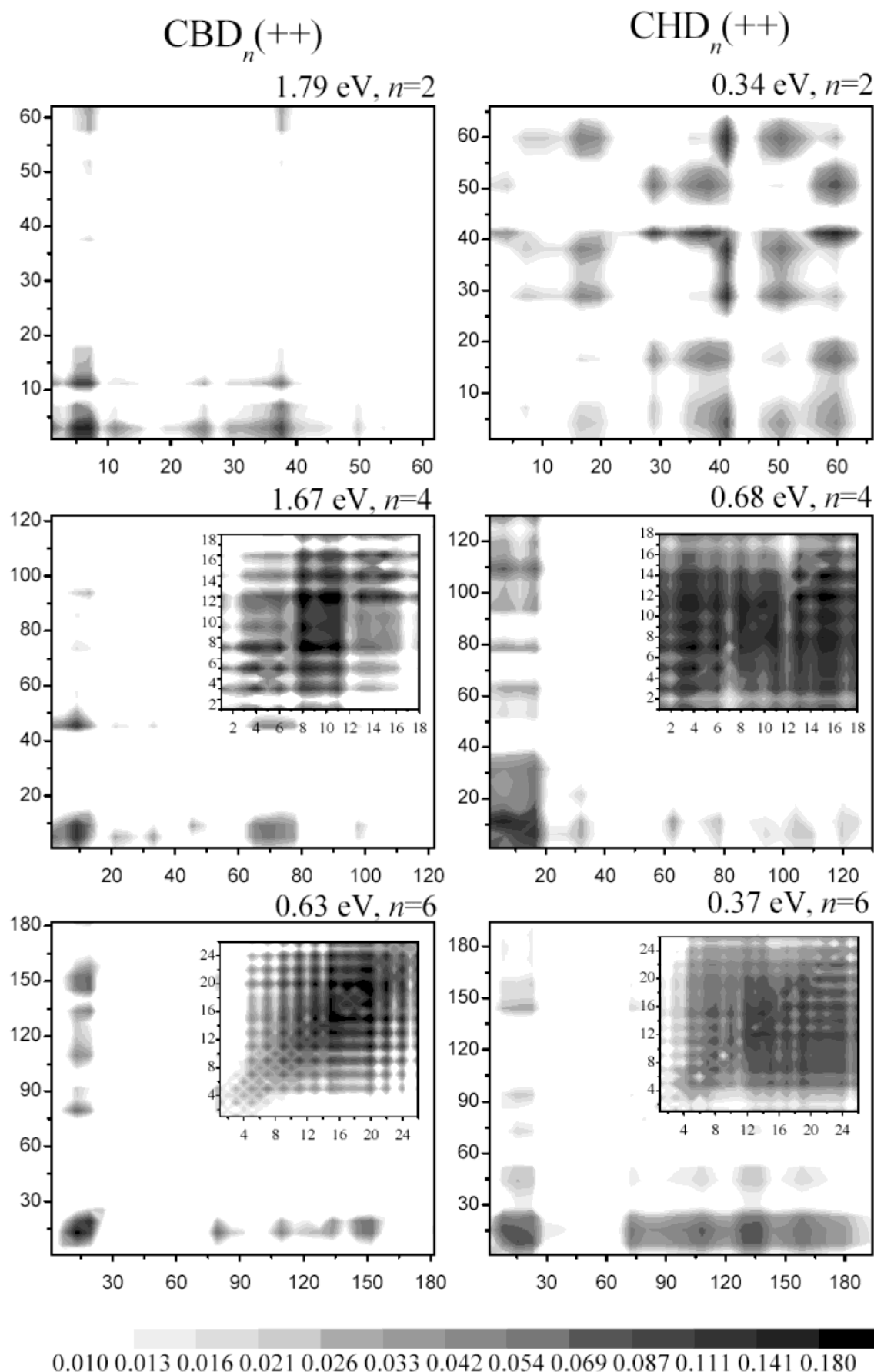


**Figure 8.** Contour plots of the CEO-modes for the lowest optical transitions of  $\text{CBD}_n$  and  $\text{CHD}_n$  doubly charged oligomers. The insets show details of the backbone region. Bottom: logarithmic contour scale. The atom labeling is shown in Figure 3.

polyDCHD<sup>30</sup> which shows two bands at  $\sim 0.1$  (broadened) and 0.81 eV. The hexamer case is not very different, but the relative oscillator strengths of the manifold of allowed low-energy transitions and of the transition at about 0.68 eV result to be inverted.

#### 4. Conclusion

In the two model systems CBD<sub>n</sub> and CHD<sub>n</sub>, we have been able to show that substituents effects are not negligible nor easily predictable, especially in the presence of an electronic excitation. In fact, although for CBD<sub>n</sub> the chemical structure itself suggests that the carbazolyl moiety can interact with the  $\pi$  electrons of the backbone via the lone pair of the N atom, the possibility of a substituent/backbone interaction in CHD<sub>n</sub> is not obvious. In the first case, the  $\pi$  systems of the substituents and of the backbone directly interact, giving rise to an alternative conjugation pathway (or maybe to a more extended conjugation). Such an effect (through-bond interaction<sup>29</sup>) is already present in the neutral oligomer, but it is emphasized when a charge is injected in the structure. On the contrary, in CHD<sub>n</sub> or similar oligomers, although the two  $\pi$  systems are not reciprocally conjugated, due to their relative orientation and small distance, an electron flow is seen to take place between them (through-space interaction<sup>29</sup>).

A further remarkable point is the difference in the nature of the excitons associated with the double charge in the unsubstituted, CBD<sub>n</sub> and CHD<sub>n</sub> oligomers, which in turn can affect the charge transport properties. In the first case, the bipolaronic structure obtained for large oligomers is reminiscent of a system of two interacting polarons.<sup>28</sup> For CBD<sub>n</sub> a bipolaronic structure independent of the oligomer size is found, whereas for CHD<sub>n</sub>, the excess charge does not give rise to any similarly relaxed structure, but rather to an interaction between the  $\pi$  system of the backbone and the partially charged carbazole moieties.

Finally, CHD<sub>n</sub> appears to represent a better model, with respect to our previous investigation,<sup>25</sup> of the nature of the photoexcitons in polyDCHD, in that the predicted low-energy excitations compare more favorably with experimental results.

**Acknowledgment.** We thank Professor S. Mukamel for the permission to use the CEO code. The research was supported by the Italian MIUR through the Fondo per gli Investimenti della Ricerca di Base (FIRB 2001–2003) project.

#### References and Notes

- (1) *Semiconducting Polymers: Chemistry, Physics and Engineering*; Hadziioanou, G.; Van Hutten, P. F., Ed.; Wiley: New York, 2000.
- (2) Friend, R. H.; Gymer, R. W.; Holmes, A. B.; Burroughs, J. H.; Marks, R. N.; Taliani, C.; Bradley, D. D. C.; Dos Santos, D. A.; Brédas, J. L.; Lögdlund, M.; Salaneck, W. R. *Nature* **1999**, *397*, 121.
- (3) Cocchi, M.; Virgili, D.; Giro, G.; Fattori, V.; Di Marco, P.; Kalinowski, J.; Shirota, Y. *Appl. Phys. Lett.* **2002**, *80*, 2401.
- (4) Pei, Q.; Yang, Y.; Yu, G.; Zhang, C.; Heeger, A. J. *J. Am. Chem. Soc.* **1996**, *118*, 3922.
- (5) Sariciftci, N. S.; Smilowitz, L.; Heeger, A. J.; Wudl, F. *Science* **1992**, *258*, 1474.
- (6) Sirringhaus, H.; Brown, P. J.; Friend, R. H.; Nielsen, M. M.; Bechgaard, K.; Langeveld-Voss, B. M. W.; Spiering, A. J. H.; Janssen, R. A. J.; Meijer, E. W.; Herwig, P.; de Leeuw, D. M. *Nature* **1999**, *401*, 685.
- (7) Granstrom, M.; Petrisch, K.; Arias, A. C.; Lux, A.; Andersson, M. R.; Friend, R. H. *Nature* **1998**, *395*, 257.
- (8) Baughman, R. H.; et al. *Science* **1999**, *284*, 1340.
- (9) Mukamel, S.; Tretiak, S.; Wagersreiter, T.; Chernyak, V. *Science* **1997**, *277*, 781.
- (10) Tretiak, S.; Chernyak, V.; Mukamel, S. *J. Phys. Chem. B* **1998**, *102*, 3310.
- (11) Shuai, S. *Phys. Rev. B* **1984**, *29*, 4570.
- (12) Grando, D.; Banfi, G. P.; Comoretto, D.; Dellepiane, G. *Chem. Phys. Lett.* **2002**, *363*, 492.
- (13) Alloisio, M.; Cravino, A.; Moggio, I.; Comoretto, D.; Bernocco, S.; Cuniberti, C.; Dell'Erba, C.; Dellepiane, G. *J. Chem. Soc., Perkin Trans.* **2001**, *2*, 146.
- (14) Dewar, M. J. S.; Zebisch, E. G.; Healy, E. F.; Steward, J. J. P. *J. Am. Chem. Soc.* **1985**, *107*, 3902.
- (15) Stewart, J. J. P. *J. Comput.-Aided Mol. Des.* **1990**, *4*, 1.
- (16) Cornil, J.; Beljonne, D.; Brédas, J. L. *J. Chem. Phys.* **1995**, *103*, 834.
- (17) Tretiak, S.; Mukamel, S. *Chem. Rev.* **2002**, *102*, 3171.
- (18) Chernyak, V.; Schulz, M. F.; Mukamel, S.; Tretiak, S.; Tsiper, E. V. *J. Chem. Phys.* **2000**, *113*, 36.
- (19) Tretiak, S.; Chernyak, V.; Mukamel, S. *J. Am. Chem. Soc.* **1997**, *119*, 11408.
- (20) Zerner, M. C.; Loew, G. H.; Kirchner, R. F.; Müller-Westerhoff, U. T. *J. Am. Chem. Soc.* **1980**, *102*, 589.
- (21) Pople, J. A.; Beveridge, D. L.; Dobosh, P. J. *Chem. Phys.* **1967**, *47*, 2026.
- (22) See Brédas, J. L.; Adant, C.; Tacks, P.; Persoons, A.; Pierce, B. M. *Chem. Rev.* **1994**, *94*, 243 and reference therein.
- (23) Ottonelli, M.; Moggio, I.; Musso, G. F.; Comoretto, D.; Cuniberti, C.; Dellepiane, G. *Synth. Met.* **2001**, *124*, 179.
- (24) Hädicke, E.; Mez, E. C.; Krauch, C. H.; Wegner, G.; Kaiser, J. *Angew. Chem.* **1971**, *83*, 253.
- (25) Ottonelli, M.; Moggio, I.; Musso, G. F.; Comoretto, D.; Cuniberti, C.; Dellepiane, G. *Synth. Met.* **2001**, *119*, 611.
- (26) Zojer, E.; Cornil, J.; Leising, G.; Brédas, J. L. *Phys. Rev. B*, **1999**, *59*, 7957.
- (27) Bäuerle, P.; Segelbacher, U.; Mainer, A.; Mehring, M. *J. Am. Chem. Soc.* **1993**, *115*, 10217.
- (28) Ottonelli, M.; Musso, G. F.; Comoretto, D.; Dellepiane, G. *Phys. Chem. Chem. Phys.* **2002**, *4*, 2754.
- (29) Ottonelli, M.; Musso, G. F.; Dellepiane, G. *App. Surf. Sci.* **2004**, *226*, 99. In this preliminary paper (relative to  $n = 4$  only), we made the exactly opposite choice with respect to the present one. That is, we reported the lowest-energy transition instead of the one having the highest oscillator strength.
- (30) Comoretto, D.; Cuniberti, C.; Musso, G. F.; Dellepiane, G.; Speroni, F.; Botta, C.; Luzzati, S. *Phys. Rev. B* **1994**, *49*, 8059.